Supplementary Material

Chemically amplified molecular resins for shrinkage-controlled direct nanoimprint lithography of functional oxides: An application towards dark-light dual-mode antibacterial surfaces

Ravikiran Nagarjuna,[a] Anindita Thakur,[b] Aniket Balapure,[a] Mohammad S. M. Saifullah,[c] Jayati Ray Dutta[b] and Ramakrishnan Ganesan*[a]*

[a] Department of Chemistry, Birla Institute of Technology and Science (BITS), Pilani, Hyderabad Campus, Jawahar Nagar, Kapra Mandal, Medchal District, Hyderabad, Telangana – 500078. India

[b] Department of Biological Sciences, Birla Institute of Technology and Science (BITS), Pilani, Hyderabad Campus, Jawahar Nagar, Kapra Mandal, Medchal District, Hyderabad, Telangana – 500078. India

c Laboratory for Micro and Nanotechnology, Paul Scherrer Institut, Forschungsstrasse 111, 5232 Villigen PSI, Switzerland

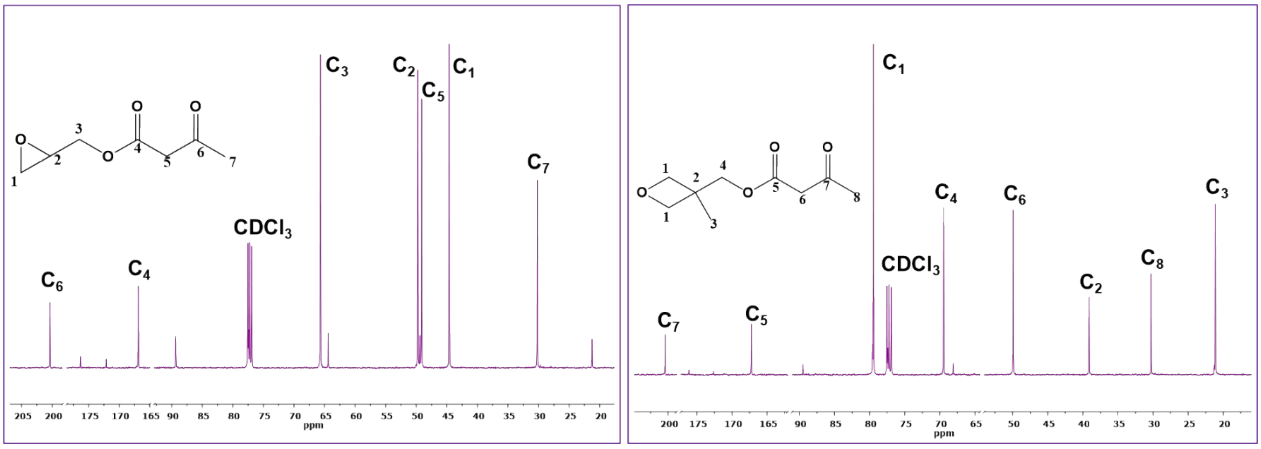

Fig. S1 ^{13}C NMR spectra of EAA (left) and OAA (right) monomers.

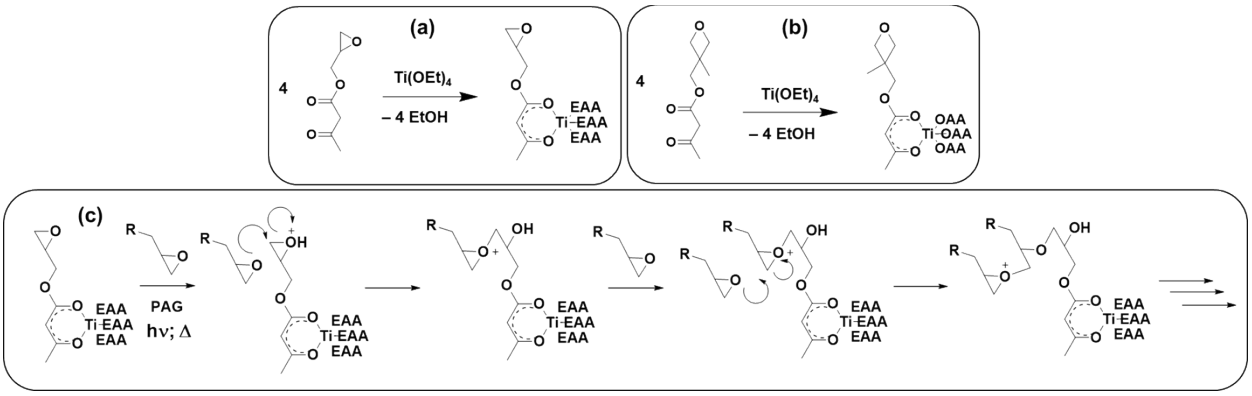

Fig. S2 Reaction of EAA and OAA with titanium (IV) ethoxide to synthesize (a) $Ti(EAA)_4$ and (b) $Ti(OAA)_4$, respectively. (c) A representative photogenerated acid-induced thermal epoxy curing reaction in $Ti(EAA)_4$ resin.

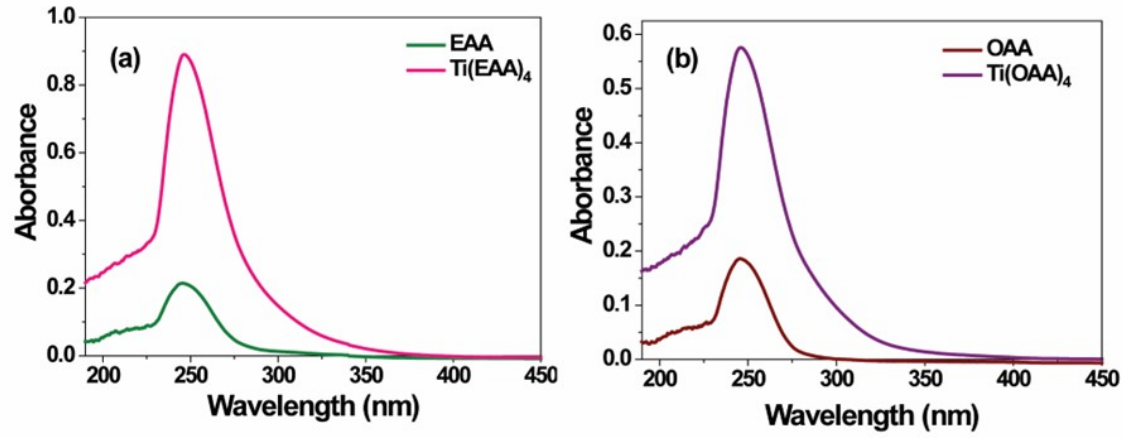

Fig. S3 UV-visible absorption spectra of the CAR-based monomers before and after complexing with titanium (IV) ethoxide in $CHCl_3$ solvent: (a) EAA and $Ti(EAA)_4$ and (b) OAA and $Ti(OAA)_4$.

The UV-Vis absorption spectra of the as-synthesized EAA and $Ti(EAA)_4$ were recorded in $CHCl_3$ solvent and the results are shown in Fig. S3(a). It can be seen from the figure that EAA showed an absorption maximum (λ_{max}) at 245.5 nm, which could be attributed to the n → π* transition arising from the keto groups of acetoacetate. Upon addition of Ti-ethoxide, the intensity of this peak was increased due to the formation of six membered ring between the metal and EAA. Besides, the absorption profile was further stretched to 350 nm, as opposed to 280 nm of the as-synthesized EAA. A similar trend was observed with OAA and $Ti(OAA)_4$ (Fig. S3(b)). These results additionally confirm the charge transfer in the metal complex due to chelation.

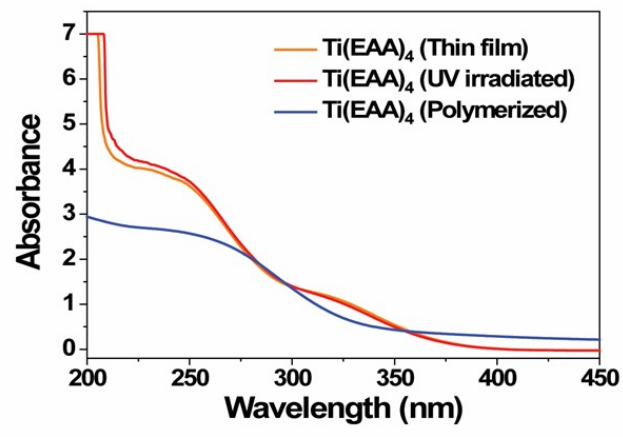

Fig. S4 UV-visible absorbance spectra of $Ti(EAA)_4$ thin film as-coated over quartz substrate and after subsequent steps like UV irradiation and PEB to induce ring opening polymerization.

The $Ti(EAA)_4$ resin was spin coated over a quartz plate and recorded with the UV-Vis spectra to observe any changes during UV irradiation and subsequent PEB step (Fig. S4). The spectrum of $Ti(EAA)_4$ shows the absorption below 250 nm is due to the chelation of the metal to the monomer. The spectrum after UV irradiation was found to be almost similar to that of the as-coated film, while the absorption was found to decrease after the polymerization step. This could be due to the local chemical changes in the polymerized film. Nevertheless, a considerable amount of absorption was found to remain even after the polymerization, indicating that the intactness of the chelated metal complex, as observed from the FT-IR studies.

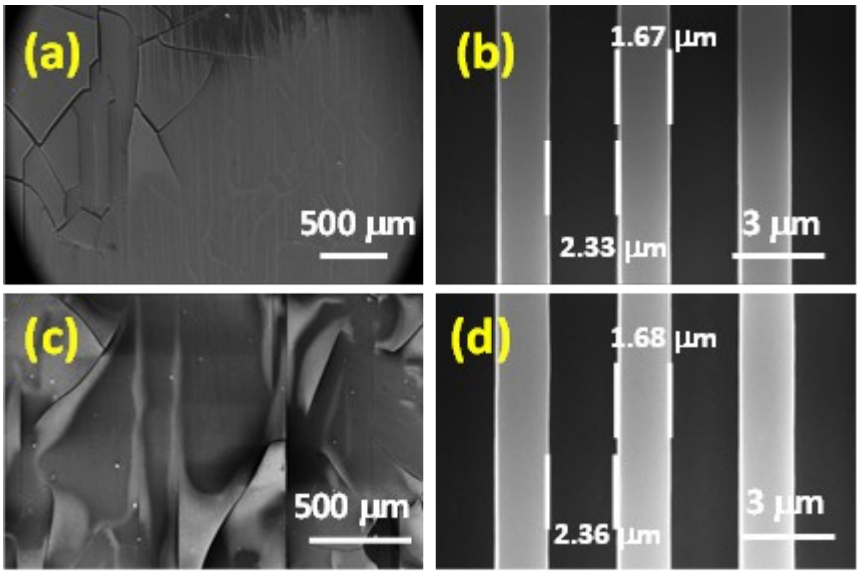

Fig. S5 FE-SEM images of the imprints (before calcination) using (a, b) $Ti(OEt)_2(EAA)_2$ and (c, d) $Ti(OEt)_2(OAA)_2$ resin formulations.

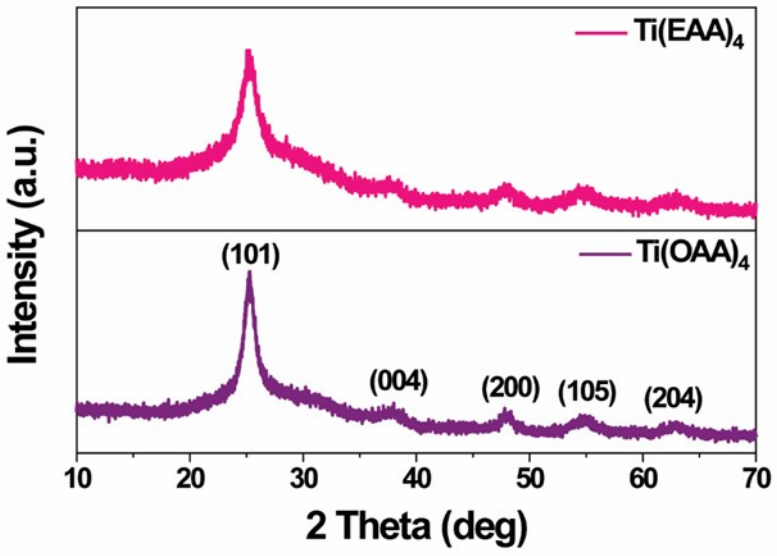

Fig. S6 XRD patterns of TiO_2 thin films obtained by calcination of polymerized thin films at 450 °C using $Ti(EAA)_4$ and $Ti(OAA)_4$ formulations.

To verify the formation of crystalline metal oxide, the films calcined at 450 °C were subjected to X-ray diffraction (XRD) measurements. Fig. S6 shows the XRD patterns of the thin films of TiO_2 prepared from $Ti(EAA)_4$ and $Ti(OAA)_4$. In both the cases phase pure anatase TiO_2 (JCPDS 89-4921) was found to be obtained after calcination. The broad peaks indicate the

nanocrystalline nature of the material. The crystallite sizes of TiO_2 in the thin films formed from $Ti(EAA)_4$ and $Ti(OAA)_4$ have been calculated using Scherrer's formula as 6.5 and 8.2 nm, respectively.

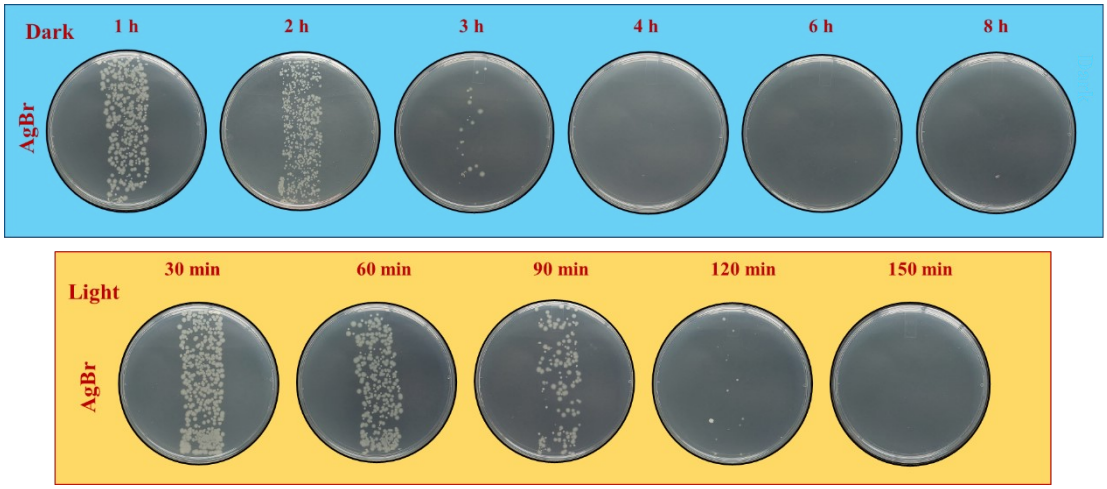

Fig. S7 Antimicrobial efficacy of the pristine AgBr coating under dark (top panel) and visible-light (bottom panel) conditions.

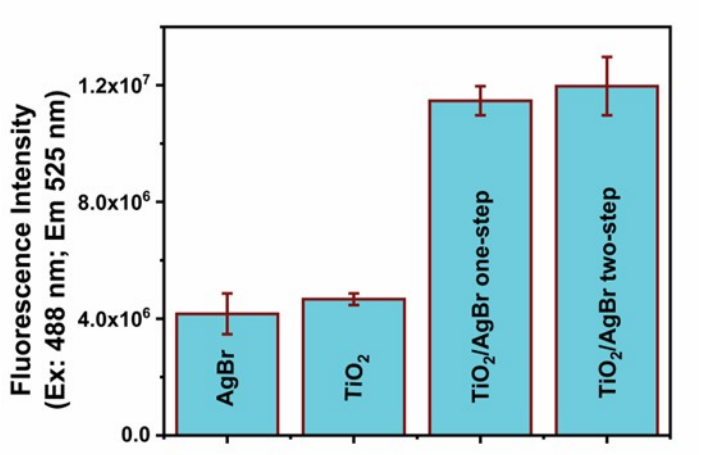

Fig. S8 Quantification of visible-light-mediated ROS generation, in the nanocomposites in comparison to the individual constituents, using DCFH-DA probe.